Development 140, 2345-2353 (2013) doi:10.1242/dev.093500

Elastogenesis at the onset of human cardiac valve development

Miriam Votteler[1,2], Daniel A. Carvajal Berrio[2], Alexander Horke[3], Laetitia Sabatier[4], Dieter P. Reinhardt[4], Ali Nsair[5], Elena Aikawa[6] and Katja Schenke-Layland[1,2,5,*]

SUMMARY

Semilunar valve leaflets have a well-described trilaminar histoarchitecture, with a sophisticated elastic fiber network. It was previously proposed that elastin-containing fibers play a subordinate role in early human cardiac valve development; however, this assumption was based on data obtained from mouse models and human second and third trimester tissues. Here, we systematically analyzed tissues from human fetal first (4-12 weeks) and second (13-18 weeks) trimester, adolescent (14-19 years) and adult (50-55 years) hearts to monitor the temporal and spatial distribution of elastic fibers, focusing on semilunar valves. Global expression analyses revealed that the transcription of genes essential for elastic fiber formation starts early within the first trimester. These data were confirmed by quantitative PCR and immunohistochemistry employing antibodies that recognize fibronectin, fibrillin 1, 2 and 3, EMILIN1 and fibulin 4 and 5, which were all expressed at the onset of cardiac cushion formation (~week 4 of development). Tropoelastin/elastin protein expression was first detectable in leaflets of 7-week hearts. We revealed that immature elastic fibers are organized in early human cardiovascular development and that mature elastin-containing fibers first evolve in semilunar valves when blood pressure and heartbeat accelerate. Our findings provide a conceptual framework with the potential to offer novel insights into human cardiac valve development and disease.

KEY WORDS: Heart, Elastin, Elastic fibers, Extracellular matrix, Heart valves

INTRODUCTION

Despite the fact that elastin and elastic fibers are pivotal for normal cardiac development and function, the majority of research efforts have not been focused on the impact of the extracellular matrix (ECM) on organogenesis or pathological remodeling processes. While recent reports on cardiac ischemia have emphasized the importance of ECM in the cardiovascular system (Barallobre-Barreiro et al., 2012), there has been little focus on the role of the ECM, in particular elastin, in human cardiovascular embryonic development.

Elastin is a non-soluble, extremely durable protein. The processes underlying elastic fiber formation are highly complex and require the interplay of various molecules. To date, the mechanisms that drive elastic fiber formation, termed ‘elastogenesis’, are not well defined but are the subject of intense research by many groups (Kielty et al., 2002a; Wagenseil and Mecham, 2007; Wise and Weiss, 2009). Elastic fibers consist of a variety of components, including microfibrillar proteins (fibrillins), linking proteins [fibulins, elastin microfibril interfacers (EMILINs), microfibril-associated glycoproteins (MAGPs)], soluble factors [e.g. transforming growth factor (TGF) beta] and the core protein elastin (Wagenseil and Mecham, 2007; Sherratt, 2009; Wise and Weiss, 2009). In addition, a fibronectin network is needed for the assembly of fibrillins, and consequently of microfibrils, that provides a microenvironment which controls tropoelastin/elastin arrangement and cross-linking processes (Sabatier et al., 2009). Fibulin 5 and MAGP1 (also known as MFAP2) are known to bridge between microfibrils and tropoelastin (Gibson et al., 1986; Nakamura et al., 2002; Yanagisawa et al., 2002; Cirulis et al., 2008). Fibulin 4 (also known as EFEMP2) links the enzyme lysyl oxidase (LOX) to tropoelastin (Horiguchi et al., 2009). Interestingly, in organisms that possess a low-pressure circulation system, microfibrils alone provide sufficient elasticity (Faury, 2001; Piha-Gossack et al., 2012). By contrast, in organisms that feature a higher blood pressure, elastin-containing fibers are required. In such systems it has been suggested that, during embryonic development, an incorporation of elastin into the microfibrillar network takes place when blood pressure increases (Faury, 2001; Wagenseil and Mecham, 2009).

As elastin is a very durable protein that can remain functional throughout a lifetime [e.g. elastin turnover in human lung is ~74 years (Shapiro et al., 1991)], gene expression is reduced in aging cardiovascular tissues (Kelleher et al., 2004; Wagenseil and Mecham, 2009). Elastic fibers provide the essential recoil for all tissues that are exposed to constant, repeated strain, such as the larger arteries or heart valve leaflets (Faury, 2001; Kielty et al., 2002b; Wagenseil and Mecham, 2007; Sherratt, 2009). In semilunar valve leaflets, the layer facing the ventricles (the ventricularis) is mainly composed of a sophisticated elastic fiber network, which is vital for physiological leaflet function (Aikawa et al., 2006; Lindsey

[1]University Women’s Hospital Tübingen and Inter-University Centre for Medical Technology Stuttgart-Tübingen (IZST), Eberhard Karls University, 72076 Tübingen, Germany. [2]Department of Cell and Tissue Engineering, Fraunhofer Institute for Interfacial Engineering and Biotechnology (IGB), 70569 Stuttgart, Germany. [3]Department of Cardiac, Thoracic, Transplantation and Vascular Surgery, Hannover Medical School, 30625 Hannover, Germany. [4]Department of Anatomy and Cell Biology, and Faculty of Dentistry, Division of Biomedical Sciences, Faculty of Medicine, McGill University, Montreal, Quebec H3A 2B2, Canada. [5]Department of Medicine/Cardiology, Cardiovascular Research Laboratories (CVRL), University of California Los Angeles (UCLA), Los Angeles, CA 90095, USA. [6]Cardiovascular Medicine, Brigham and Women's Hospital, Harvard Medical School, Boston, MA 02115, USA.

*Author for correspondence (katja.schenke-layland@med.uni-tuebingen.de)

Accepted 3 April 2013

and Butcher, 2011; Schenke-Layland et al., 2004). However, the mechanisms underlying this specialized histoarchitectural assembly are poorly understood and neither the endogenous (e.g. cellular and ECM involvement) nor exogenous (e.g. biophysical signals) contribution is sufficiently defined.

It was suggested that elastin-containing fibers are first detectable at the onset of the third trimester in developing human valves (Aikawa et al., 2006). In that study, only routine histological analyses were performed by employing Verhoeff's elastic stain, which is the elastic fiber-detecting stain within the Russel-Movat pentachrome stain (Movat's stain). However, Verhoeff's elastic stain is only suitable to visualize mature elastic fibers (Mulisch and Welsch, 2010) and it does not detect early, non-cross-linked fibers or microfibrils. Therefore, we aimed in this study to employ antibody and probe-specific analyses to identify the temporal and spatial distribution of the early elastic fiber network in developing human hearts with a focus on the semilunar valves.

MATERIALS AND METHODS

Human heart valve tissue procurement and processing

This study was performed in accordance with institutional guidelines and was approved by the local research ethics committees at the University of California Los Angeles (UCLA) and the University Hospital of the Eberhard Karls University (UKT) (UCLA IRB #05-10-093; UKT IRB #356/2008BO2 and #406/2011BO1). First trimester (n=8; 4-12 weeks of gestation) and second trimester (n=7; 13-18 weeks of gestation) human fetal hearts were obtained from electively aborted fetuses. Cryopreserved adult aortic valves from adolescents (n=5; 14-19 years) and adults (n=5; 50-55 years), which were not suitable for transplantation due to extended storage times, were obtained from Cell and Tissue Systems (Prof. K. G. Brockbank, Charleston, SC, USA). After either harvest or thawing procedures, all tissues were immediately washed in sterile phosphate-buffered saline (PBS) (Lonza, Cologne, Germany), fixed in 10% buffered formalin for less than 12 hours, then rinsed in tap water and transferred to 70% ethanol. Fixed specimens were embedded in paraffin.

Laser-capture microdissection (LCM) and RNA isolation

LCM of formalin-fixed paraffin-embedded (FFPE) samples was performed as previously described (Votteler et al., 2013). Dissected leaflets and large outflow tract vessels were collected separately in adhesive caps (Carl Zeiss, Jena, Germany). RNA was then extracted using an isolation kit specific for FFPE samples (#74404 and #73504, RNeasy FFPE Kit, Qiagen, Hilden, Germany). For cryopreserved tissues, we separated leaflets and the aortic trunk by tweezers and extracted RNA using the Microarray RNeasy Kit (#76163, Qiagen). All further processing was performed according to the manufacturer's protocols. The purified RNA was eluted in RNase-free water and stored at −80°C until gene expression analyses.

Whole-genome expression analyses

Microarrays were performed by MFTServices (UKT) using the cDNA-mediated annealing, selection, extension and ligation (DASL) assay (Illumina, San Diego, CA, USA) for RNA of FFPE and cryopreserved tissues as previously described (Fan et al., 2004). RNA quality was monitored using microfluidics-based electrophoresis (BioAnalyzer 2100, Agilent, Waldbronn, Germany) and spectrophotometric analysis (Nanodrop ND-1000, PEQLAB Biotechnologie, Erlangen, Germany). For data processing and analyses, Genome Studio V2009.1 software (Illumina) was used. The expression data from all chips were normalized with variance stabilizing normalization (VSN). Heatmaps were created with R (http://www.r-project.org) and vertical scatterplots were designed using GraphPad Prism 5 software (GraphPad Software, La Jolla, CA, USA). All data are displayed as intensities ($\log_2$ normalized ratios) ± s.d. Microarray data have been deposited at GEO with accession number GSE45821.

Histology

Movat's stain was used to visualize mature elastin-containing elastic fibers (black), nuclei (dark red), collagens (yellow), muscle tissue (red) and proteoglycans (blue-green) as previously described (Russell, 1972; Aikawa et al., 2006; Schenke-Layland et al., 2008).

Immunofluorescence staining and imaging

Tissue sections (3 μm) were deparaffinized and all slides were processed as previously described (Schenke-Layland et al., 2007). Antigen retrieval was performed in a microwave oven for 8 minutes each in 10 mM Tris, 1 mM EDTA, 0.05% Tween 20 (pH 9.0) and in 10 mM citrate solution in PBS (pH 6.0). All sections were then incubated for 30 minutes in blocking buffer (2% goat serum, 0.1% Triton X-100, 0.05% Tween 20 in PBS). Antibodies were diluted in blocking buffer without goat serum. Primary antibodies were polyclonal rabbit IgG anti-elastin (1:75) and anti-EMILIN1 (1:500) Prestige antibodies (#HPA018111 and #HPA002822, Sigma-Aldrich, Munich, Germany) and anti-fibronectin (1:500; #A0245, Dako, Eching, Germany). Anti-fibrillin 1, 2 and 3 (each 1:1000) and anti-fibulin 4 and 5 (each 1:500) were produced in rabbits (Lin et al., 2002; Sabatier et al., 2011). Primary antibodies were incubated overnight at 4°C. Alexa Fluor 594-conjugated goat anti-rabbit IgG (H+L) secondary antibodies (Life Technologies, Molecular Probes, Darmstadt, Germany) were diluted 1:250 and applied for 30 minutes at room temperature. For co-labeling we employed FITC-labeled α-smooth muscle actin (αSMA) (1:400; #F3777, Sigma-Aldrich). After incubation with secondary antibodies, slides were exposed to 4′,6-diamidino-2-phenylindole (DAPI) solution for 10 minutes followed by mounting using ProLong Gold antifade mounting medium (Life Technologies, Molecular Probes). Fluorescence images were acquired using an Axio Observer Z1 microscope or an LSM710 inverted confocal microscope (both Carl Zeiss). Images were processed with Photoshop CS5 (Adobe Systems, San Jose, CA, USA).

For semi-quantification of tropoelastin/elastin protein expression in adolescent and adult valve tissue sections, we used identical exposure times and compared gray value intensity (GVI) signals of antibody-stained tissue sections at 20× magnification as previously described (Aikawa et al., 2006; Schenke-Layland et al., 2010). For each sample group we used three sections of three specimens (n=3) and, within each section, we measured three regions of interest (ROIs).

Real-time quantitative PCR (qPCR)

qPCR of FFPE RNA was performed using a QuantiFast Probe One-Step Assay (Hs_ELN_1_FAM, Qiagen). We employed 10 ng total RNA and used the recommended cycling conditions (95°C for 3 minutes, followed by 45 cycles at 95°C for 3 seconds and 60°C for 30 seconds). All data are displayed as arbitrary units (a.u.).

Statistical analyses

Statistical significance was determined by ANOVA with Tukey's multiple comparison tests and Student's t-test using GraphPad Prism 5 software. $P<0.05$ was defined as statistically significant.

RESULTS

Human fetal first trimester cardiovascular structures exhibit elastin-containing fibers at 4 weeks of development

It has been reported that elastin-containing fibers and the typical trilaminar architecture are first seen in developing human semilunar valves after 36 weeks of gestation, as detected using Movat's stain (Aikawa et al., 2006). Our study confirmed these results and also showed no evidence for elastin and elastin-containing fibers in human first trimester (4-12 weeks) semilunar valve leaflets using Movat's stain (Fig. 1A,D, blue arrow). However, using targeted antibody staining, we detected tropoelastin/elastin-containing fiber structures in human developing valves as early as 7 weeks of gestation (Fig. 1B). Interestingly, a rudimentary stratification was already visible at this early stage of valve development, as tropoelastin/elastin was mainly expressed in the layer facing the ventricles (Fig. 1B, arrows).

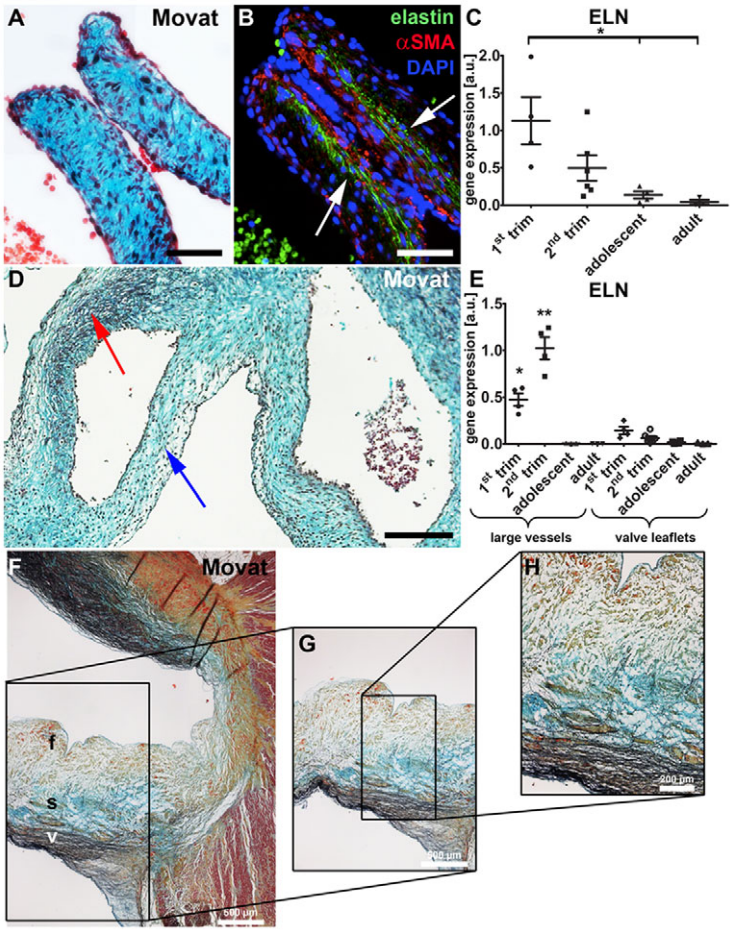

Fig. 1. Routine histology and probe-specific analyses identify tropoelastin/elastin gene and protein expression patterns in human semilunar valve leaflets. (**A**,**B**) Routine histology (A; Movat's stain) and immunofluorescence staining with an antibody against tropoelastin/elastin (B; green) of a 9-week human fetal semilunar valve leaflet section. In B, DAPI-stained nuclei are in blue and α-smooth muscle actin (αSMA)-expressing cells are in red. Arrows indicate tropoelastin/elastin in the layer facing the ventricles. (**C**) qPCR data of *ELN* expression; **P*<0.05, first trimester versus adolescent and adult tissues. Error bars indicate s.d. (**D**) Movat's stain of an 11-week tissue section showing the fetal outflow tract [red arrow points to elastic fibers (black) within the large arteries]. By contrast, no elastin-containing fibers are visible in the semilunar leaflet (blue arrow). (**E**) qPCR data comparing *ELN* expression in developing large outflow tract vessels and leaflets. **P*<0.05, first trimester large vessels versus adolescent and adult vessels and all valve groups; ***P*<0.05, second trimester large vessels versus all vessel and valve groups. (**F-H**) Adult (50 years) aortic valve leaflet stained with Movat's stain. f, fibrosa; s, spongiosa; v, ventricularis. Scale bars: 50 μm in A,B; 200 μm in D,H; 500 μm in F,G.

Quantitative real-time PCR data revealed that elastin (*ELN*) gene expression decreases in semilunar valve leaflets with increasing age. Accordingly, we detected a significant decrease in adolescent and adult tissues when compared with the first trimester samples [12.1±8.6% adolescent versus first trimester (set to 100%), $P<0.02$; 3.7±5% adult versus first trimester (set to 100%), $P<0.03$] (Fig. 1C). This decrease in *ELN* expression with age was also seen in the large vessels. The elastin content was significantly lower in the valve leaflets than in the large vessels both on the protein and gene level (Fig. 1D,E). In addition to *ELN* expression being significantly higher in the vascular structures during early gestation, we also observed earlier maturation of the elastic fibers in the fetal large vessels, as Movat's stain detected elastin-containing elastic fibers already within the first trimester (Fig. 1D, red arrow). These results are similar to reports focusing on the developing heart in chicken, where elastic fiber components were detectable using immunofluorescence staining in the early embryonic outflow tract, but not in age-matched cardiac valves (Hurle et al., 1994). In adult semilunar valve leaflets, routine histology was suitable to visualize the complex network of elastin-containing fibers within the ventricularis layer of semilunar leaflets (Fig. 1F-H, black staining).

Microfibril and associated proteins are expressed at the onset of human semilunar valve cushion development

Previous studies have hypothesized that elastogenesis starts with microfibril formation followed by elastin deposition (Kielty et al., 2002a; Wagenseil and Mecham, 2007). Cross-linking mechanisms complete the maturation process of elastic fibers (Kielty et al., 2002a; Wagenseil and Mecham, 2007). In order to identify whether microfibril-associated proteins are present in developing valves, we isolated RNA from semilunar valve leaflets of first and second trimester hearts employing LCM. We compared the fetal tissues with tissues ranging from 14-19 (adolescent) and 50-55 (adult) years. We performed global gene expression analyses and identified that key microfibril-associated protein genes required for elastic fiber assembly were highly expressed as early as the first trimester: fibronectin (*FN1*), fibrillin 2 and 3 (*FBN2* and *FBN3*), *MAGP1*, latent transforming growth factor beta binding protein 1, 3 and 4 (*LTBP1*, *3* and *4*), *LOX*, fibulin 2, 4 and 5 (*FBLN2*, *4* and *5*) and *EMILIN1* (Fig. 2). Clustering analyses further revealed that some of these genes, such as *FBN2* and *FBN3*, are highly expressed during fetal development, but then significantly diminished in adolescent and adult valves: *FBN2* and *FBN3* were the most highly expressed during fetal development [respectively: 13.4±0.3 and 12.2±0.4 first trimester; 13.2±0.2 and 11.4±0.6 second trimester; Fig. 2 (red)] and decreased significantly with increasing age [respectively: 8.4±0.8 and 6.2±0.4 adolescent; 8.2±1.5 and 5.9±0.8 adult; Fig. 2 (green); $P<0.05$].

Other genes, including *FN1*, *LTBP4*, *LOX*, *FBLN2*, *FBLN4*, *FBLN5* and *EMILIN1*, are expressed throughout life, although a statistically significant decrease was seen for most of the genes. For example, *EMILIN1* and *FN1* were overall highly expressed (respectively: 12.3±0.3 and 11.6±0.5 first trimester; 12.1±0.2 and 11.5±0.3 second trimester; 10.7±0.6 and 10.3±0.6 adolescent; 10.7±0.2 and 10.3±0.1 adult). *FBN1* showed low expression throughout life, with a significant decrease in aging valves (9.2±0.4 first trimester; 9.1±0.3 second trimester; 7.6±0.5 adolescent; 7.8±0.3 adult; $P<0.05$).

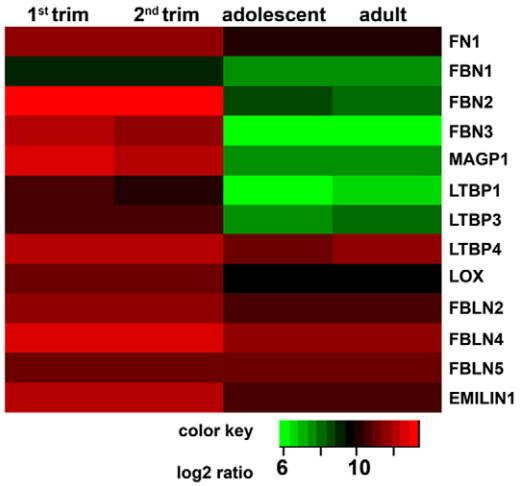

Fig. 2. Genome-wide transcriptional profiling to determine age-related gene expression changes in semilunar valves. Low expression, green; high expression, red.

Protein expression analyses (Fig. 3; supplementary material Fig. S1) revealed that fibronectin, as well as fibrillin 1, 2 and 3, were detectable throughout the entire cushion area of the semilunar valves at embryonic week 4 (Fig. 3A,D,G,J). By contrast, with the beginning of leaflet elongation within the first trimester, fibronectin and fibrillin 1 and 2 were increasingly detectable within the ventricularis layer (Fig. 3B,E,H). Fibrillin 3 was predominantly visible within the basement membrane (Fig. 3H), a spatial pattern previously reported in human epithelia and endothelia (Sabatier et al., 2011). Interestingly, in mature leaflets, fibrillin 1 was not exclusively located in the ventricularis, but also spread into the spongiosa (Fig. 3C). Similar to the *FBN2* expression profile, fibrillin 2 was not detectable by immunofluorescence staining in adolescent and adult tissues (Fig. 3I).

Differential spatiotemporal expression of elastin-associated proteins and tropoelastin/elastin in human fetal, adolescent and adult semilunar valve leaflets

In addition to microfibrillar proteins, we analyzed proteins that are associated with tropoelastin/elastin deposition and required for cross-linking processes (Fig. 4; supplementary material Fig. S1). We also explored the expression patterns of the core protein elastin (Figs 5 and 6; supplementary material Fig. S1). Overall, protein expression analyses revealed the differential distribution of EMILIN1, fibulin 4 and 5 in aging valves. EMILIN1 was found throughout the 4-week-old cushions (Fig. 4A) and became more restricted to the ventricularis layer at 9 weeks (Fig. 4B). In adolescent and adult leaflets, EMILIN1 was detectable in both the ventricularis and spongiosa (Fig. 4C). By contrast, fibulin 4 was expressed equivalently in developing and aged semilunar valves and was predominantly located within the ventricularis and spongiosa leaflet layers (Fig. 4D-F). Although fibulin 5 was initially detectable throughout the entire leaflet and became spatially restricted to the ventricularis layer, similar to the expression pattern observed for EMILIN1 (Fig. 4G,H), it was highly expressed within the ventricularis with increasing age (Fig. 4I). Gene expression analyses showed significantly decreasing *FBLN4* levels in adolescent and adult leaflets when compared with first and second trimester tissues (92±4.5% adolescent and 91.8±0.9% adult; $P<0.001$), whereas *FBLN5* expression remained constant throughout the lifetime (Fig. 2).

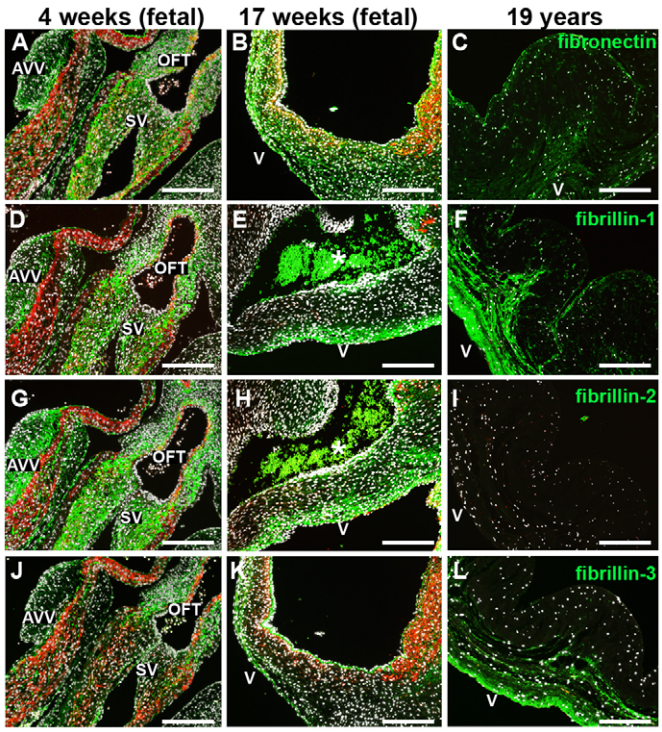

Fig. 3. Microfibrillar proteins are expressed at the onset of semilunar cushion formation. Immunofluorescence staining of human semilunar valve tissues of different developmental stages (4 weeks, early first trimester; 17 weeks, second trimester; 19 years, adolescent) reveals the expression patterns of microfibrillar proteins (green) including fibronectin (**A-C**), fibrillin 1 (**D-F**), fibrillin 2 (**G-I**) and fibrillin 3 (**J-L**). DAPI-stained nuclei are white and αSMA-expressing cells are red. Asterisks indicate erythrocytes. AVV, atrioventricular valves; SV, semilunar valves; OFT, outflow tract; v, ventricularis. Scale bars: 200 μm.

Tropoelastin/elastin deposition was first seen in the vasculature of the outflow tract of 4-week-old fetal hearts (Fig. 5A,B, arrow). The frequency of elastin-containing elastic fibers had rapidly increased by week 5-6 (Fig. 5C, arrow). In semilunar valves, tropoelastin/elastin expression appeared temporally distinct from that in the vascular structures. The earliest elastic fibers were detectable within the ventricularis layer at week 7 of human fetal development (Fig. 5D, arrow). Interestingly, at 9 weeks, a network of elastic fibers was predominantly seen in the ventricularis (Fig. 5E). At 15 weeks of development, elastin-containing elastic fibers were mainly observed in the ventricularis layer, close to the vessel wall (Fig. 5F).

Tropoelastin/elastin was expressed throughout the entire ventricularis layer in adolescent and adult valve leaflets (Fig. 6A,B). In addition to the quantitative gene expression analysis (Fig. 1C), we performed semi-quantification of antibody-stained tissue sections. Here, we identified a significant decrease in tropoelastin/elastin protein expression with increasing age (a 42.8±7.2% decrease in adult tissues compared with adolescent samples; $P=0.0004$; Fig. 6C).

DISCUSSION

In this study, we showed for the first time that tropoelastin/elastin expression in human developing hearts starts considerably earlier

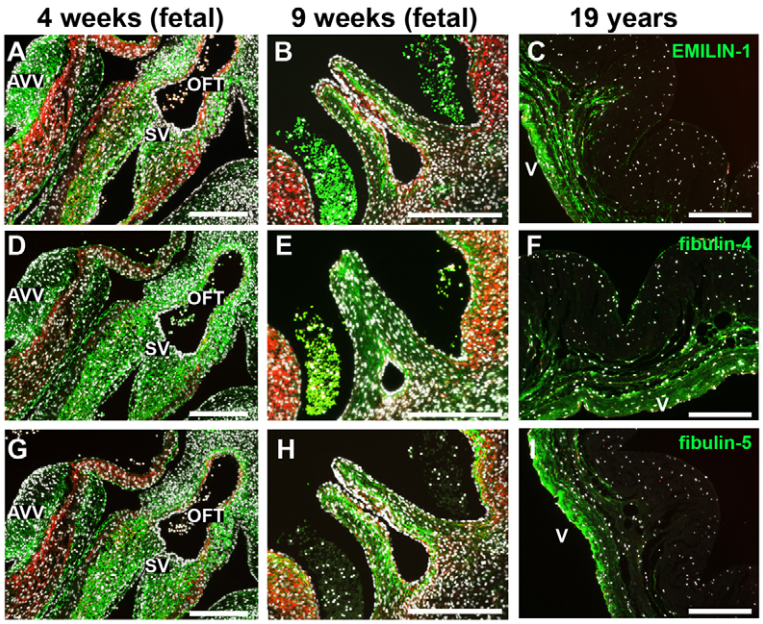

Fig. 4. Human semilunar cushion matrix is rich in elastin fiber components EMILIN1, fibulin 4 and fibulin 5. Immunofluorescence imaging of valve leaflet sections at the indicated developmental stages stained for EMILIN1 (**A-C**), fibulin 4 (**D-F**) and fibulin 5 (**G-I**) shows differences in the protein expression patterns (all in green). DAPI-stained nuclei are white and αSMA-positive cells are red. Asterisks indicate erythrocytes. AVV, atrioventricular valves; SV, semilunar valves; OFT, outflow tract; v, ventricularis. Scale bars: 200 μm.

than previously projected (Aikawa et al., 2006). The earliest tropoelastin/elastin patterns were detectable in the outflow tract vasculature of the developing 4-week human heart, at a time when the heart first starts to beat, the blood pressure is marginal and the vessel wall is exposed for the first time to shear stress. During human fetal development, the heartbeat starts at the beginning of week 4 with a frequency of ~65 beats per minute (bpm), which accelerates in week 7 when it peaks at 180 bpm (Riem Vis et al., 2011). It might be speculated that, for the proper development of an elastic fiber network, the peak seen at 7 weeks of human development is the cue for elastin production in semilunar valves; however, this would not explain the early presence of tropoelastin/elastin in the outflow tract vasculature, which raises questions as to whether the cues for vascular and valvular tropoelastin/elastin deposition are similar.

It had been hypothesized in mouse models that elastin production might be impacted by changes in hemodynamic forces (Wagenseil et al., 2010). The amount of elastin in large arteries was seen to increase significantly at mouse developmental stage E18, which is approximately equivalent to the third trimester in humans. The increase in pressure at this stage of development (E18-P1) was reported to be a key signal for fibrillogenesis and elastin-containing fiber assembly. It was further proposed that these ontogenetic changes are similar to phylogenetic changes in ECM expression patterns in the vasculature of invertebrates (<20-30 mm Hg) as compared with vertebrates (>20 mm Hg) (Faury, 2001; Kelleher et al., 2004; Wagenseil et al., 2010; Cheng and Wagenseil, 2012). Immunofluorescence analyses in chicken have revealed that tropoelastin expression starts at embryonic stages HH21-22 in the outflow tract vessels and that the formation of an elastic layer wall starts between HH22 and HH29, which is equivalent to ~4-6 weeks of gestation in humans; the first signs of elastogenesis in chicken cardiac valves appeared comparatively delayed, at HH30 (equivalent to ~6 weeks gestation in humans) (Hurle et al., 1994; Little and Rongish, 1995; Lindsey and Butcher, 2011).

The major aim of this study was to identify the dynamic expression patterns of microfibril and associated proteins as well as of elastin and, ultimately, to define the earliest appearance of elastic fibers in human semilunar valves. Using antibodies and specific probes, we demonstrated that most of the proteins required for the assembly of an elastic fiber network were present in semilunar cushions as early as 4 weeks of human development. Tropoelastin/elastin deposition was first detectable at 7 weeks, during the period of morphogenic transition from the cushion stage to the elongated leaflet structure. Interestingly, it appeared that the stratified histoarchitecture of the semilunar valve leaflet, with elastic fibers being predominantly located within the ventricularis, was already predetermined between weeks 7 and 9 of gestation. By contrast, Movat's stain, with Verhoeff's stain revealing the elastic fibers, was not appropriate to visualize elastin and these early elastin-containing fibers, similar to findings previously described by others (Aikawa et al., 2006; Lindsey and Butcher, 2011). Indeed, it has been reported that Verhoeff's elastic stain is not suitable to detect immature elastic fibers (Mulisch and Welsch, 2010). It appears that the histological dye fails to detect immature elastin-containing microfibrillar structures in early tissues due to the lack of cross-links, which occur later in development (third trimester) when the fibers mature. We conclude that ECM-visualizing stains, such as Movat's, that contain Verhoeff's stain are suitable to detect mature ECM components but fail to identify developing, immature ECM structures.

In this study, we present the first comprehensive expression analysis of elastogenesis, both on the gene and protein level, providing unique insights into elastogenesis in human developing and aging semilunar valve tissues. Fibrillin 1 showed completely different protein and gene expression patterns to fibrillin 2 and 3. Fibrillin 2 and fibrillin 3 were mainly expressed during fetal development and decreased significantly in postnatal life, whereas fibrillin 1 protein was detected throughout all developmental stages. These results are consistent with the proposition that fibrillin 2 regulates the early process of elastic fiber assembly, whereas fibrillin 1 provides structural and force-bearing support, making continued fibrillin 1 deposition a premise for the maturation of fully functional cardiovascular tissues (Zhang et al., 1995; Carta et al., 2006). In addition, our data suggest that fibrillin 2 is generally produced during valve development and remodeling, whereas fibrillin 1 production continues after birth, which is similar to

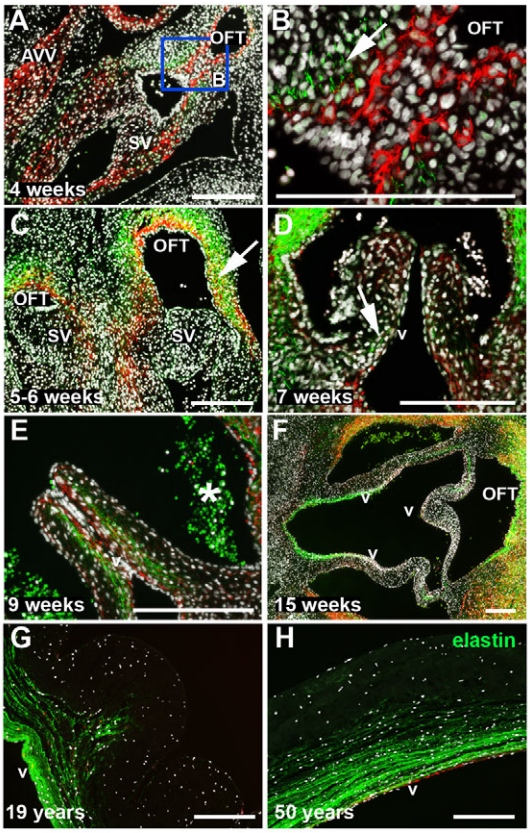

Fig. 5. Tropoelastin/elastin protein expression is first seen in the outflow tract vasculature of 4-week hearts and can be visualized with a 3-week delay in semilunar valve leaflets. Immunofluorescence images of tropoelastin/elastin (green) expression in fetal (**A-F**), adolescent (**G**) and adult (**H**) cardiac tissues, with focus on the semilunar valves that are localized in the outflow tract. The boxed region in A is shown at higher magnification in B. DAPI-stained nuclei are white and αSMA-expressing cells are red. Arrows point to elastin-containing fibers. Asterisks indicate erythrocytes. AVV, atrioventricular valves; OFT, outflow tract; SV, semilunar valve; v, ventricularis. Scale bars: 200 μm.

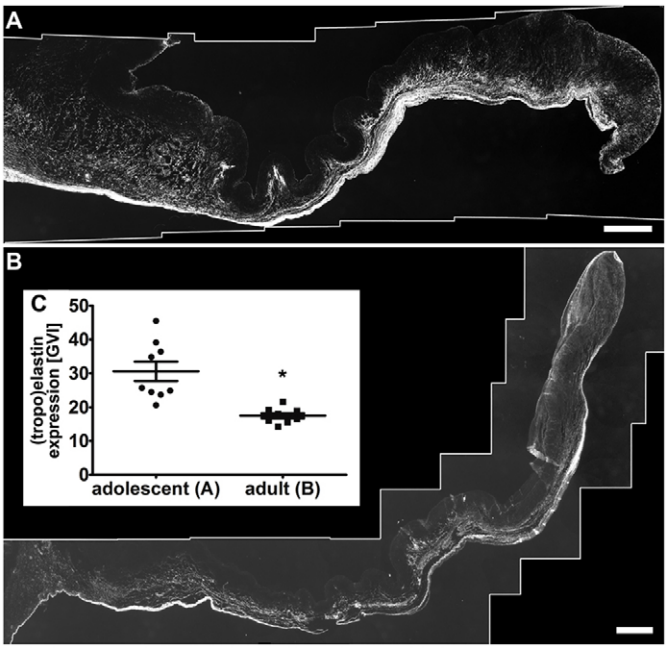

Fig. 6. Tropoelastin/elastin content decreases significantly within aging valve leaflets. (**A**,**B**) Representative immunofluorescence images of adolescent (A) and adult (B) aortic heart valve leaflets showing tropoelastin/elastin expression patterns (white). Scale bars: 500 μm. (**C**) Semi-quantification of tropoelastin/elastin protein expression based on gray value intensities (GVI). *P=0.0004, adolescent versus adult tissues. Error bars indicate s.d.

previous reports in other organ systems (Zhang et al., 1995; Kelleher et al., 2004; Carta et al., 2006). The function of fibrillin 3 has not yet been determined (Sabatier et al., 2011); however, our gene expression analysis confirmed the data of Sabatier et al. that, similar to fibrillin 2, fibrillin 3 is highly expressed during fetal cardiac development and is significantly decreased in postnatal life. Additionally, we observed that fibrillin 3 protein expression was predominantly within the basement membrane of semilunar valve leaflets.

In addition to microfibril-associated proteins, we detected the presence of proteins required for tropoelastin/elastin deposition and integration into microfibrils, such as fibulin 4 and 5 and EMILIN1, in the early stages of human semilunar cushion formation. Both fibulin 4 and 5 assist tropoelastin aggregation and transfer to the extracellular space as well as facilitating elastin deposition on microfibrils (Nakamura et al., 2002; Yanagisawa et al., 2002; Cirulis et al., 2008; Horiguchi et al., 2009; Yanagisawa and Davis, 2010). Here, we revealed that, in aging valve leaflets, only fibulin 5 was constantly expressed in the ventricularis. It had been reported that EMILIN1 is found on the interface between the amorphous elastin core and microfibrils (Bressan et al., 1993; Wagenseil and Mecham, 2007). Although our results showed that tropoelastin/elastin and EMILIN1 indeed exhibited similar gene and protein expression patterns throughout life, with colocalization in the ventricularis and areas of the spongiosa, EMILIN1 was already detectable throughout the cushions of 4-week hearts, whereas tropoelastin/elastin was not yet detectable in these early semilunar valves (compare Fig. 4A with Fig. 5A,C).

It had been suggested that elastin protein is predominantly produced and deposited during fetal and neonatal development and that it lasts throughout the lifetime without replacement (Kelleher et al., 2004; Sherratt, 2009; Wagenseil and Mecham, 2012). Our data confirmed that elastin expression is significantly decreased in semilunar valves with increasing age. We further revealed that tropoelastin/elastin protein expression started at week 7 in semilunar valve leaflets and that towards the end of the first trimester a network of elastin-containing fibers was seen in the developing ventricularis layer. An elastic fiber system with fibers branching out to connect to the fibrosa, a pattern that was previously described in the porcine system (Tseng and Grande-Allen, 2011), was seen thereafter and into postnatal life. However, semi-quantification of the antibody-stained tissue sections revealed significantly decreasing amounts of tropoelastin/elastin protein with increasing age.

When considering the hypothesis that biophysical signals are essential for elastogenesis, it was interesting to identify that tropoelastin/elastin protein was first detectable in the outflow tract vasculature of 4-week fetal human hearts, when the heartbeat begins and the blood pressure starts to increase (Faury, 2001; Riem Vis et al., 2011). In species with low-pressure circulation systems, microfibrils are known to provide sufficient elasticity and strength

Table 1. Elastin and elastic fiber protein expression in human developing semilunar valves and the diseases associated with these proteins

Protein	Expression in semilunar valves				Associated diseases
	4-6 weeks	7+ weeks	Adolescent	Adult	
fibronectin	++	+	+	+	–
fibrillin 1	++	++	++	++	Marfan syndrome (Ramirez, 1996)
fibrillin 2	++	++	–	–	Beals syndrome (Putnam et al., 1995)
fibrillin 3	+	+	+	+	–
fibulin 4	+	+	+	+	Cutis laxa (Loeys et al., 1993)
fibulin 5	++	++	++	++	Cutis laxa (Loeys et al., 2002)
EMILIN1	+	++	++	++	–
(tropo)elastin	–	+	++	++	Supravalvular aortic stenosis (Curran et al., 1993), Williams-Beuren syndrome (Ewart et al., 1993), cutis laxa (Tassabehji et al., 1998), valve calcification (Aikawa et al., 2009; Perrotta et al., 2011)

–, no expression; +, expression; ++, strong expression.

within the cardiovascular system. Species with high blood pressure require the support of highly resilient proteins such as elastin (Faury, 2001). To date, elastin has only been found in vertebrates and some jawless fish [e.g. lamprey (Piha-Gossack et al., 2012)] with high blood pressure and pulsatile blood flow, which indicates that a certain threshold has to be reached to 'induce' elastin expression (Faury, 2001; Cheng and Wagenseil, 2012; Piha-Gossack et al., 2012). However, it is unknown whether immature elastin tissue structures can mature by exposure to defined biophysical signals, what these signals are and how they could be recapitulated (e.g. in a bioreactor system to engineer a cardiac valve). For almost two decades, scientists have been aiming to deliver a clinically relevant living tissue-engineered valve that is able to respond to growth and physiological forces in the same way as a native valve (Vesely, 2005), in order that it would be suitable for surgical valve reconstruction in children. To date, the only clinical experience with tissue-engineered valves resulted in a number of early failures and even patient death (Vesely, 2005). It therefore remains essential to improve our knowledge of early human cardiac valve development and the mechanisms that drive this process. Studying nature's blueprint, as in this study, the use of computational tools and the utilization of sophisticated human-based *in vitro* systems will enable greater progress towards the goal of successfully translating scientific findings into a fully functional tissue-engineered valve that can become a clinical reality.

Evidence in recent years has implicated that pathological matrix remodeling plays a key role in cardiovascular disease development, including valve calcification, which is the most common reason for surgical aortic valve replacement. Accordingly, it had been shown that ECM structural damage impacts valve durability, leading to allograft degeneration (Schenke-Layland et al., 2009; Lisy et al., 2010). Moreover, it was demonstrated that macrophage metalloproteinase (MMP12)-mediated degradation of elastic fibers contributes to valve mineralization by inducing calcium deposition onto fragmented elastin, which was identified as the initial site of calcification (Perrotta et al., 2011). Emerging evidence suggests that elastin degradation contributes to arterial and aortic valve calcification via the action of macrophage-derived cathepsin S, a highly potent elastase (Aikawa et al., 2009). Mutations in *ELN* and microfibril-associated protein genes are known to cause a variety of congenital cardiovascular diseases (Table 1), including Marfan, Beals and Williams-Beuren syndromes, as well as cutis laxa (Curran et al., 1993; Ewart et al., 1993; Loeys et al., 1993; Putnam et al., 1995; Ramirez, 1996; Tassabehji et al., 1998; Loeys et al., 2002; Aikawa et al., 2009; Perrotta et al., 2011).

Conclusions

Here, we demonstrated that elastic fiber formation starts at the onset of human semilunar valve development. Both gene and protein expression of fibronectin, fibrillins, fibulin 4 and 5 and EMILIN1 were detectable in developing semilunar valve cushions as early as week 4 of gestation. In addition, we demonstrated that tropoelastin/elastin expression starts in the outflow tract vasculature in the 4-week fetal heart and is then followed by deposition in the semilunar valve leaflets as early as week 7 of gestation, which is substantially earlier than previously projected based on data obtained from mouse models and human second and third trimester tissues. Based on previous reports, the hypothesis was raised that elastin and elastic fibers might not be crucial for early cardiovascular organ development. By contrast, our study, which provided unique insights into the evolution of the human cardiovascular system, demonstrates that elastin and elastic fibers are important for the development of functional semilunar leaflets, providing a conceptual framework to further identify the mechanisms that tightly control cardiovascular tissue morphogenesis and homeostasis.

Because we utilized non-diseased human tissues in this study, we were limited to descriptive analyses that do not allow functional insight into the process of elastogenesis. Although we identified interspecies differences between data obtained from previous mouse experiments and our findings in the human system, in-depth mechanistic analyses of the semilunar valve tissues of the elastin knockout mouse (Wagenseil et al., 2010) might further elucidate general molecular events involved in valvulogenesis. In future studies, it will be essential to investigate the impact of microenvironmental cues on the interactions between cells and with the ECM, soluble factors and biophysical signals that allow elastogenesis. Our findings might provide novel insights into therapies for acquired and congenital cardiovascular disease.

Acknowledgements

We thank Simone Liebscher and Susanne Geist (University Women's Hospital Tübingen) for assistance with immunofluorescence staining; Kai Pusch (Fraunhofer IGB Stuttgart) and the MFT Services core facility (UKT) for the performance of gene expression arrays; and Prof. Dr Kelvin G. Brockbank (Cell and Tissue Systems, Charleston, SC, USA) for providing tissues. Special acknowledgment is given to Shannon Lee Layland (Fraunhofer IGB Stuttgart) for outstanding support in the gene expression analyses and constructive thoughts on the manuscript.

Funding

We are grateful for financial support by the Fraunhofer-Gesellschaft [Attract 692263 to K.S.-L.]; the Bundesministerium für Bildung und Forschung (BMBF)

[0316059 to K.S.-L.]; the Ministry of Science, Research and the Arts of Baden-Württemberg [33-729.55-3/214 to K.S.-L.]; and the Canadian Institutes of Health Research and the Natural Sciences and Engineering Research Council of Canada (both to D.P.R.). Deposited in PMC for immediate release.

Competing interests statement

The authors declare no competing financial interests.

Supplementary material

Supplementary material available online at
http://dev.biologists.org/lookup/suppl/doi:10.1242/dev.093500/-/DC1

References

Aikawa, E., Whittaker, P., Farber, M., Mendelson, K., Padera, R. F., Aikawa, M. and Schoen, F. J. (2006). Human semilunar cardiac valve remodeling by activated cells from fetus to adult: implications for postnatal adaptation, pathology, and tissue engineering. *Circulation* **113**, 1344-1352.

Aikawa, E., Aikawa, M., Libby, P., Figueiredo, J. L., Rusanescu, G., Iwamoto, Y., Fukuda, D., Kohler, R. H., Shi, G. P., Jaffer, F. A. et al. (2009). Arterial and aortic valve calcification abolished by elastolytic cathepsin S deficiency in chronic renal disease. *Circulation* **119**, 1785-1794.

Barallobre-Barreiro, J., Didangelos, A., Schoendube, F. A., Drozdov, I., Yin, X., Fernández-Caggiano, M., Willeit, P., Puntmann, V. O., Aldama-López, G., Shah, A. M. et al. (2012). Proteomics analysis of cardiac extracellular matrix remodeling in a porcine model of ischemia/reperfusion injury. *Circulation* **125**, 789-802.

Bressan, G. M., Daga-Gordini, D., Colombatti, A., Castellani, I., Marigo, V. and Volpin, D. (1993). Emilin, a component of elastic fibers preferentially located at the elastin-microfibrils interface. *J. Cell Biol.* **121**, 201-212.

Carta, L., Pereira, L., Arteaga-Solis, E., Lee-Arteaga, S. Y., Lenart, B., Starcher, B., Merkel, C. A., Sukoyan, M., Kerkis, A., Hazeki, N. et al. (2006). Fibrillins 1 and 2 perform partially overlapping functions during aortic development. *J. Biol. Chem.* **281**, 8016-8023.

Cheng, J. K. and Wagenseil, J. E. (2012). Extracellular matrix and the mechanics of large artery development. *Biomech. Model. Mechanobiol.* **11**, 1169-1186.

Cirulis, J. T., Bellingham, C. M., Davis, E. C., Hubmacher, D., Reinhardt, D. P., Mecham, R. P. and Keeley, F. W. (2008). Fibrillins, fibulins, and matrix-associated glycoprotein modulate the kinetics and morphology of in vitro self-assembly of a recombinant elastin-like polypeptide. *Biochemistry* **47**, 12601-12613.

Curran, M. E., Atkinson, D. L., Ewart, A. K., Morris, C. A., Leppert, M. F. and Keating, M. T. (1993). The elastin gene is disrupted by a translocation associated with supravalvular aortic stenosis. *Cell* **73**, 159-168.

Ewart, A. K., Morris, C. A., Atkinson, D., Jin, W., Sternes, K., Spallone, P., Stock, A. D., Leppert, M. and Keating, M. T. (1993). Hemizygosity at the elastin locus in a developmental disorder, Williams syndrome. *Nat. Genet.* **5**, 11-16.

Fan, J. B., Yeakley, J. M., Bibikova, M., Chudin, E., Wickham, E., Chen, J., Doucet, D., Rigault, P., Zhang, B., Shen, R. et al. (2004). A versatile assay for high-throughput gene expression profiling on universal array matrices. *Genome Res.* **14**, 878-885.

Faury, G. (2001). Function-structure relationship of elastic arteries in evolution: from microfibrils to elastin and elastic fibres. *Pathol. Biol. (Paris)* **49**, 310-325.

Gibson, M. A., Hughes, J. L., Fanning, J. C. and Cleary, E. G. (1986). The major antigen of elastin-associated microfibrils is a 31-kDa glycoprotein. *J. Biol. Chem.* **261**, 11429-11436.

Horiguchi, M., Inoue, T., Ohbayashi, T., Hirai, M., Noda, K., Marmorstein, L. Y., Yabe, D., Takagi, K., Akama, T. O., Kita, T. et al. (2009). Fibulin-4 conducts proper elastogenesis via interaction with cross-linking enzyme lysyl oxidase. *Proc. Natl. Acad. Sci. USA* **106**, 19029-19034.

Hurle, J. M., Kitten, G. T., Sakai, L. Y., Volpin, D. and Solursh, M. (1994). Elastic extracellular matrix of the embryonic chick heart: an immunohistological study using laser confocal microscopy. *Dev. Dyn.* **200**, 321-332.

Kelleher, C. M., McLean, S. E. and Mecham, R. P. (2004). Vascular extracellular matrix and aortic development. *Curr. Top. Dev. Biol.* **62**, 153-188.

Kielty, C. M., Sherratt, M. J. and Shuttleworth, C. A. (2002a). Elastic fibres. *J. Cell Sci.* **115**, 2817-2828.

Kielty, C. M., Wess, T. J., Haston, L., Ashworth, J. L., Sherratt, M. J. and Shuttleworth, C. A. (2002b). Fibrillin-rich microfibrils: elastic biopolymers of the extracellular matrix. *J. Muscle Res. Cell Motil.* **23**, 581-596.

Lin, G., Tiedemann, K., Vollbrandt, T., Peters, H., Batge, B., Brinckmann, J. and Reinhardt, D. P. (2002). Homo- and heterotypic fibrillin-1 and -2 interactions constitute the basis for the assembly of microfibrils. *J. Biol. Chem.* **277**, 50795-50804.

Lindsey, S. E. and Butcher, J. T. (2011). The cycle of form and function in cardiac valvulogenesis. *Aswan Heart Centre Science & Practice Series* **2011**, doi: 10.5339/ahcsps.2011.10.

Lisy, M., Pennecke, J., Brockbank, K. G., Fritze, O., Schleicher, M., Schenke-Layland, K., Kaulitz, R., Riemann, I., Weber, C. N., Braun, J. et al. (2010). The performance of ice-free cryopreserved heart valve allografts in an orthotopic pulmonary sheep model. *Biomaterials* **31**, 5306-5311.

Little, C. D. and Rongish, B. J. (1995). The extracellular matrix during heart development. *Experientia* **51**, 873-882.

Loeys, B., De Paepe, A. and Urban, Z. (1993). EFEMP2-related cutis laxa. In *GeneReviews* (ed. R. A. Pagon, T. D. Bird, C. R. Dolan, K. Stephens and M. P. Adam). Seattle, WA: University of Washington.

Loeys, B., Van Maldergem, L., Mortier, G., Coucke, P., Gerniers, S., Naeyaert, J. M. and De Paepe, A. (2002). Homozygosity for a missense mutation in fibulin-5 (FBLN5) results in a severe form of cutis laxa. *Hum. Mol. Genet.* **11**, 2113-2118.

Mulisch, M. and Welsch, U. (2010). *Romeis Mikroskopische Technik*. Heidelberg: Spektrum Akademischer Verlag.

Nakamura, T., Lozano, P. R., Ikeda, Y., Iwanaga, Y., Hinek, A., Minamisawa, S., Cheng, C. F., Kobuke, K., Dalton, N., Takada, Y. et al. (2002). Fibulin-5/DANCE is essential for elastogenesis in vivo. *Nature* **415**, 171-175.

Perrotta, I., Russo, E., Camastra, C., Filice, G., Di Mizio, G., Colosimo, F., Ricci, P., Tripepi, S., Amorosi, A., Triumbari, F. et al. (2011). New evidence for a critical role of elastin in calcification of native heart valves: immunohistochemical and ultrastructural study with literature review. *Histopathology* **59**, 504-513.

Piha-Gossack, A., Sossin, W. and Reinhardt, D. P. (2012). The evolution of extracellular fibrillins and their functional domains. *PLoS ONE* **7**, e33560.

Putnam, E. A., Zhang, H., Ramirez, F. and Milewicz, D. M. (1995). Fibrillin-2 (FBN2) mutations result in the Marfan-like disorder, congenital contractural arachnodactyly. *Nat. Genet.* **11**, 456-458.

Ramirez, F. (1996). Fibrillln mutations in Marfan syndrome and related phenotypes. *Curr. Opin. Genet. Dev.* **6**, 309-315.

Riem Vis, P. W., Kluin, J., Sluijter, J. P., van Herwerden, L. A. and Bouten, C. V. (2011). Environmental regulation of valvulogenesis: implications for tissue engineering. *Eur. J. Cardiothorac. Surg.* **39**, 8-17.

Russell, H. K., Jr (1972). A modification of Movat's pentachrome stain. *Arch. Pathol.* **94**, 187-191.

Sabatier, L., Chen, D., Fagotto-Kaufmann, C., Hubmacher, D., McKee, M. D., Annis, D. S., Mosher, D. F. and Reinhardt, D. P. (2009). Fibrillin assembly requires fibronectin. *Mol. Biol. Cell* **20**, 846-858.

Sabatier, L., Miosge, N., Hubmacher, D., Lin, G., Davis, E. C. and Reinhardt, D. P. (2011). Fibrillin-3 expression in human development. *Matrix Biol.* **30**, 43-52.

Schenke-Layland, K., Riemann, I., Opitz, F., König, K., Halbhuber, K. J. and Stock, U. A. (2004). Comparative study of cellular and extracellular matrix composition of native and tissue engineered heart valves. *Matrix Biol.* **23**, 113-125.

Schenke-Layland, K., Angelis, E., Rhodes, K. E., Heydarkhan-Hagvall, S., Mikkola, H. K. and Maclellan, W. R. (2007). Collagen IV induces trophoectoderm differentiation of mouse embryonic stem cells. *Stem Cells* **25**, 1529-1538.

Schenke-Layland, K., Xie, J., Angelis, E., Starcher, B., Wu, K., Riemann, I., MacLellan, W. R. and Hamm-Alvarez, S. F. (2008). Increased degradation of extracellular matrix structures of lacrimal glands implicated in the pathogenesis of Sjögren's syndrome. *Matrix Biol.* **27**, 53-66.

Schenke-Layland, K., Stock, U. A., Nsair, A., Xie, J., Angelis, E., Fonseca, C. G., Larbig, R., Mahajan, A., Shivkumar, K., Fishbein, M. C. et al. (2009). Cardiomyopathy is associated with structural remodelling of heart valve extracellular matrix. *Eur. Heart J.* **30**, 2254-2265.

Schenke-Layland, K., Xie, J., Magnusson, M., Angelis, E., Li, X., Wu, K., Reinhardt, D. P., Maclellan, W. R. and Hamm-Alvarez, S. F. (2010). Lymphocytic infiltration leads to degradation of lacrimal gland extracellular matrix structures in NOD mice exhibiting a Sjögren's syndrome-like exocrinopathy. *Exp. Eye Res.* **90**, 223-237.

Shapiro, S. D., Endicott, S. K., Province, M. A., Pierce, J. A. and Campbell, E. J. (1991). Marked longevity of human lung parenchymal elastic fibers deduced from prevalence of D-aspartate and nuclear weapons-related radiocarbon. *J. Clin. Invest.* **87**, 1828-1834.

Sherratt, M. J. (2009). Tissue elasticity and the ageing elastic fibre. *Age (Dordr.)* **31**, 305-325.

Tassabehji, M., Metcalfe, K., Hurst, J., Ashcroft, G. S., Kielty, C., Wilmot, C., Donnai, D., Read, A. P. and Jones, C. J. (1998). An elastin gene mutation producing abnormal tropoelastin and abnormal elastic fibres in a patient with autosomal dominant cutis laxa. *Hum. Mol. Genet.* **7**, 1021-1028.

Tseng, H. and Grande-Allen, K. J. (2011). Elastic fibers in the aortic valve spongiosa: a fresh perspective on its structure and role in overall tissue function. *Acta Biomater.* **7**, 2101-2108.

Vesely, I. (2005). Heart valve tissue engineering. *Circ. Res.* **97**, 743-755.

Votteler, M., Layland, S. L., Lill, G., Brockbank, K. G. M., Horke, A. and Schenke-Layland, K. (2013). RNA isolation from fetal and adult human tissues for transcriptional profiling. *Biotechnol. J.* **8**, 338-344.

Wagenseil, J. E. and Mecham, R. P. (2007). New insights into elastic fiber assembly. *Birth Defects Res. C Embryo Today* **81**, 229-240.

Wagenseil, J. E. and Mecham, R. P. (2009). Vascular extracellular matrix and arterial mechanics. *Physiol. Rev.* **89**, 957-989.
Wagenseil, J. E. and Mecham, R. P. (2012). Elastin in large artery stiffness and hypertension. *J. Cardiovasc. Transl. Res.* **5**, 264-273.
Wagenseil, J. E., Ciliberto, C. H., Knutsen, R. H., Levy, M. A., Kovacs, A. and Mecham, R. P. (2010). The importance of elastin to aortic development in mice. *Am. J. Physiol. Heart Circ. Physiol.* **299**, H257-H264.
Wise, S. G. and Weiss, A. S. (2009). Tropoelastin. *Int. J. Biochem. Cell Biol.* **41**, 494-497.
Yanagisawa, H. and Davis, E. C. (2010). Unraveling the mechanism of elastic fiber assembly: The roles of short fibulins. *Int. J. Biochem. Cell Biol.* **42**, 1084-1093.
Yanagisawa, H., Davis, E. C., Starcher, B. C., Ouchi, T., Yanagisawa, M., Richardson, J. A. and Olson, E. N. (2002). Fibulin-5 is an elastin-binding protein essential for elastic fibre development in vivo. *Nature* **415**, 168-171.
Zhang, H., Hu, W. and Ramirez, F. (1995). Developmental expression of fibrillin genes suggests heterogeneity of extracellular microfibrils. *J. Cell Biol.* **129**, 1165-1176.